FLOW AROUND XBT2D AIRPLANE WITH A 2,000 POUND G.P. BOMB

REPORT NO. N-47

Hydrodynamics Laboratory

CALIFORNIA INSTITUTE OF TECHNOLOGY PASADENA CALIFORNIA

U.S. NAVY BUREAU OF ORDNANCE CONTRACT NOrd 9612

NAVY DEPARTMENT

BUREAU OF ORDNANCE

CONTRACT NOrd 9612

FLOW AROUND XBT2D AIRPLANE WITH A 2,000 POUND G.P. BOMB

ROBERT T. KNAPP

DIRECTOR

HYDRODYNAMICS LABORATORY

CALIFORNIA INSTITUTE OF TECHNOLOGY

PASADENA, CALIFORNIA

Laboratory Report No. N-47

February 20, 1948

Report Prepared by

Gerald B. Robison

Hydraulic Engineer

Copy No. 53

CONTENTS

FLOW AROUND XBT2D AIRPLANE

WITH A 2,000 POUND G. P. BOMB

HISTORICAL SUMMARY AND AUTHORIZATION OF TESTS

Flight tests of the XBT2D-1 Airplane with 2,000 pound G. P. Bomb externally attached to the fuselage resulted in serious buffeting at critical air speeds. In a memorandum from the Bureau of Ordnance, U. S. Navy, dated 13 May, 1946, the Hydrodynamics Laboratory at the California Institute of Technology was requested to make Polarized Light Flume studies and cavitation tests on a model. The object of the tests was, originally, to obtain information helpful in eliminating such buffeting.

Independent tests conducted by the Douglas Aircraft Company, Incorporated indicated to them that the airplane buffeting was caused by vibration of the bomb tail which, in turn, was believed to be caused by the critical Mach number being reached in the region between the bomb and fuselage resulting in flow separation of an unstable nature. A new aft end section was designed and constructed by this company which further streamlined the afterbody, materially stiffened the fins, and eliminated the box type of tail. Flight tests indicated that considerably higher speeds could then be obtained before objectionable buffeting occurred. Other tests made by them indicated that the static stability of the projectile was somewhat reduced. The Douglas Aircraft Company, Incorporated furnished the following results of their tests to the Hydrodynamics Laboratory:

Configuration	Maximum Speed as Limited by Objectionable Buffeting
Clean	450 mi/hr
Std. 2,000 lb. Bomb with Mark 10 Bands	400 mi/hr
Std. 2,000 lb. Bomb with welded lugs in place of Mark 10 Bands	420 mi/hr
Std. 2,000 lb. Bomb with lugs and stiffened fins	440 mi/hr
Std. 2,000 lb. Bomb with lugs and no fins	470 + mi/hr
Std. 2,000 lb. Bomb with Douglas fins and mounting bands	460 + mi/hr

In view of the information obtained by them as to the cause and reduction of difficulties encountered, the object of further tests of a model by the Hydrodynamics Laboratory was considered to include a determination of the suitability of investigating high-velocity air flow problems in water tunnels for similar future problems as well as test of this specific model.

DESCRIPTION OF MODEL

The Douglas Aircraft Company, Inc. furnished drawings of the airplane and bomb from which a model was constructed to a scale of 1:32. A new and suitable method of mounting such a model in the Polarized Light Flume and High Speed Water Tunnel was devised. The model included those portions of the fuselage, wings, bomb and bomb appurtenances (struts, lugs, ejector) as were believed pertinent to the tests. Figure 1 is an outline drawing of the model but with full-scale (prototype) dimensions shown. Figure 2 is a drawing of the bomb with full-scale dimensions. Figure 3 shows three views of the model. The upper two are head-on and side presentations, respectively, showing the general relationship of the bomb and airplane. The bottom picture shows more detail of the airflow inlet and outlet. Figure 4 is another detail photograph of the position of the bomb and its relation to the airflow outlet.

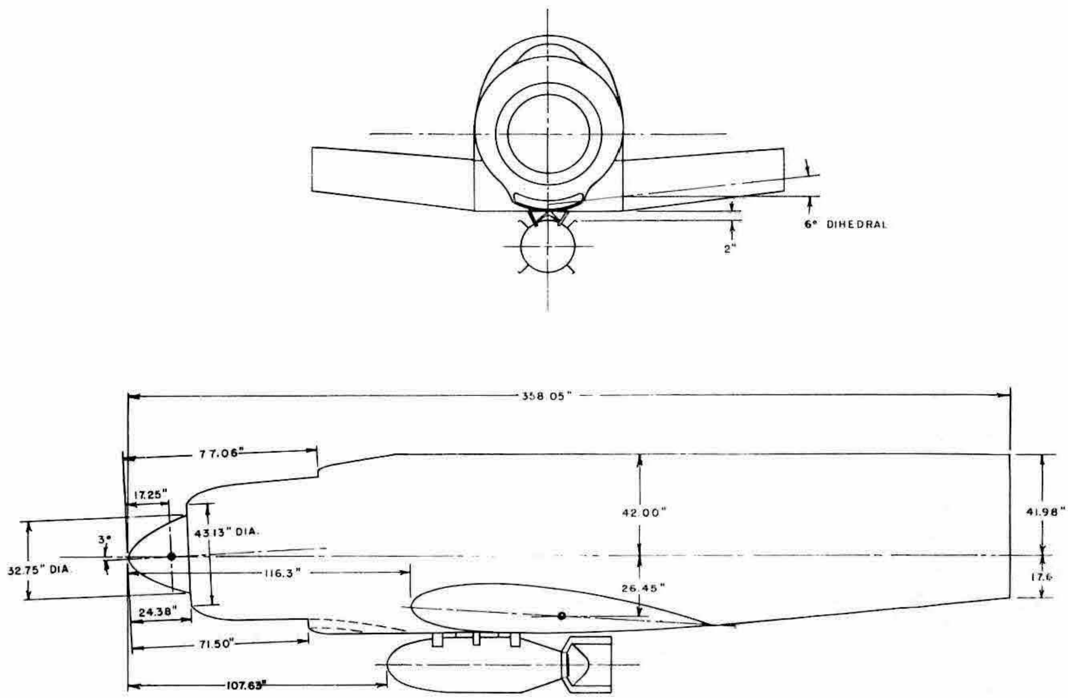

FIG. 1 — OUTLINE OF MODEL OF AIRPLANE AND BOMB
WITH PROTOTYPE DIMENSIONS

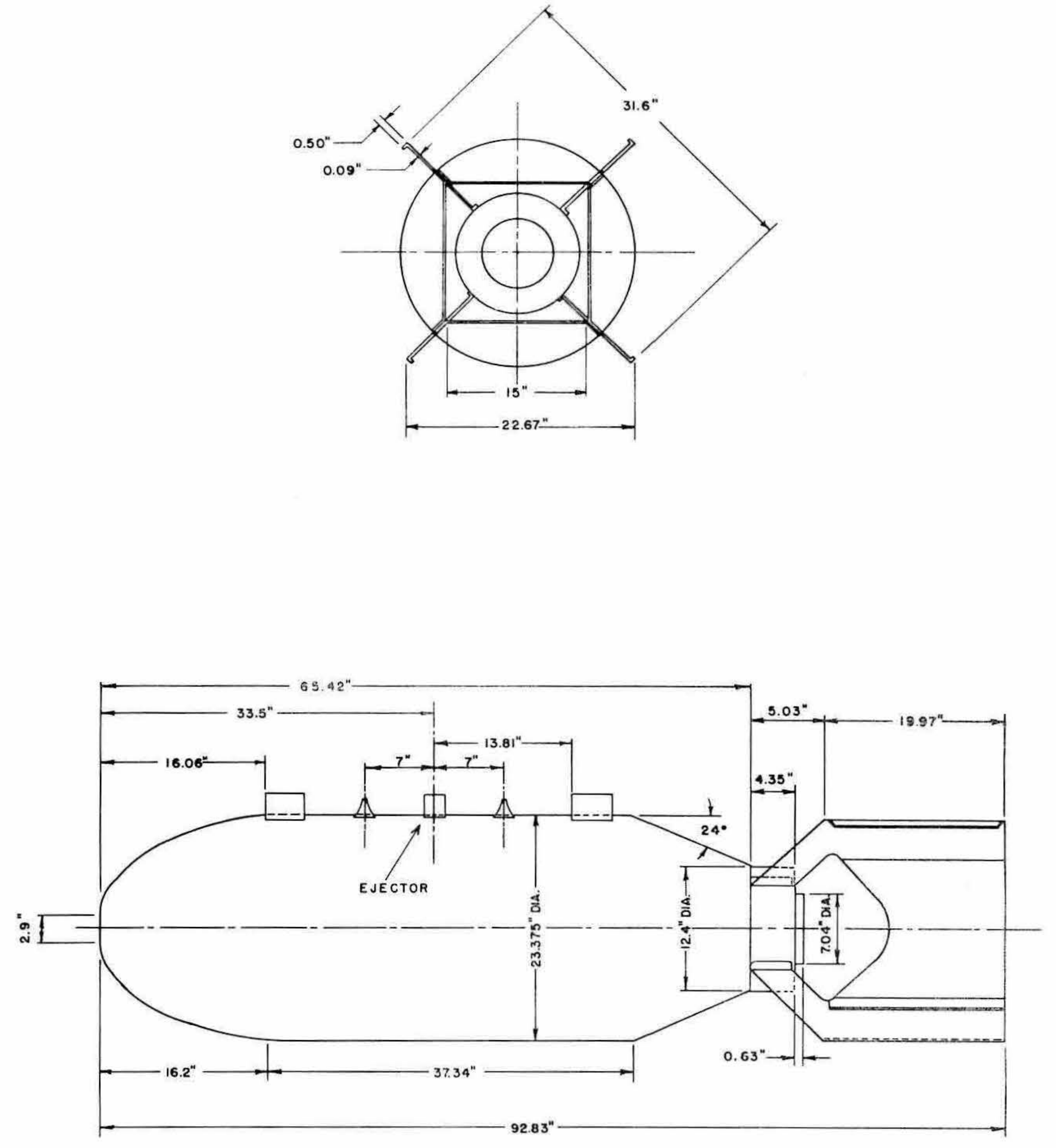

FIG. 2 — OUTLINE OF BOMB
FULL-SCALE DIMENSIONS

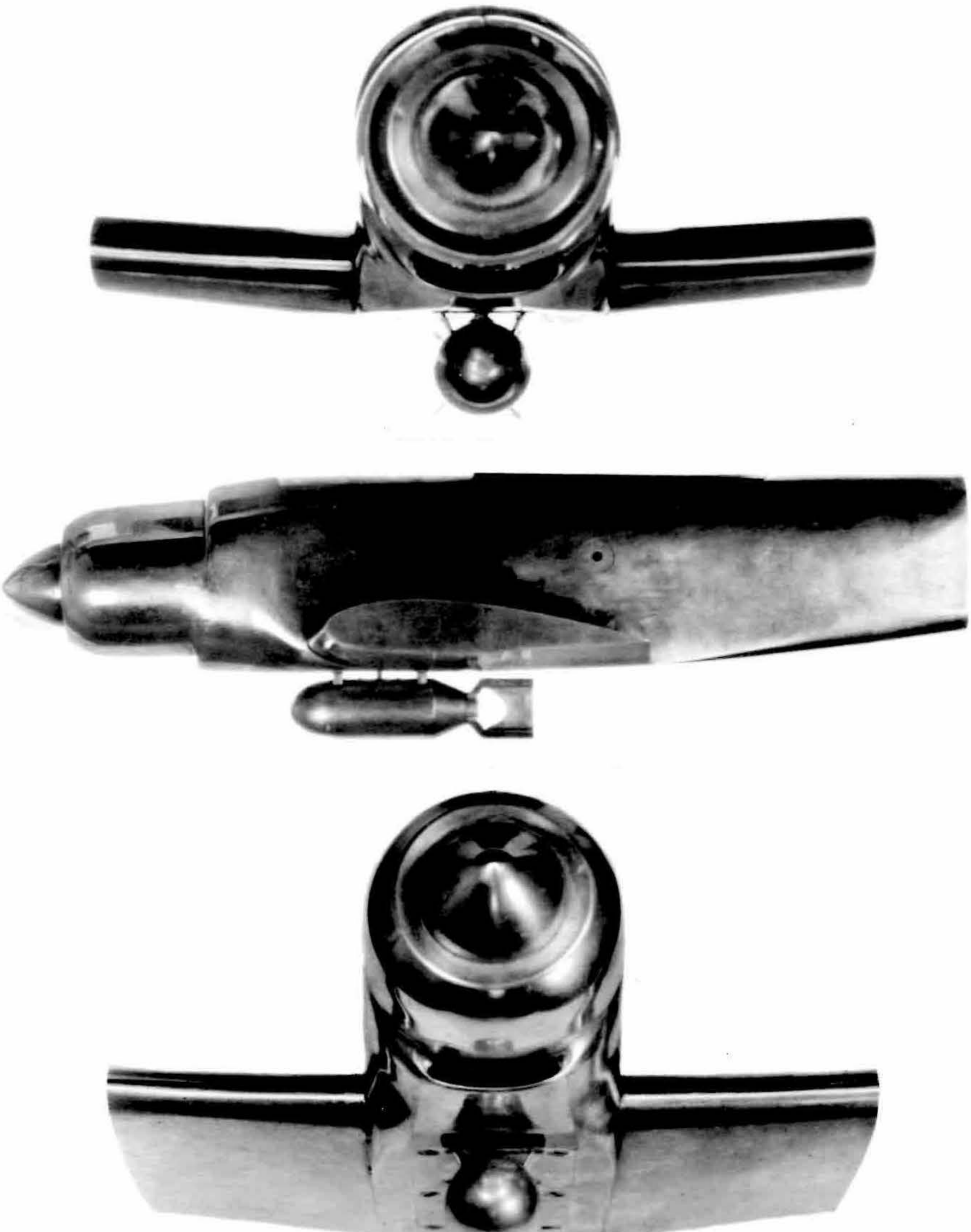

FIG. 3 – MODEL OF XBT2D-1 AIRPLANE WITH 2,000 LB. BOMB

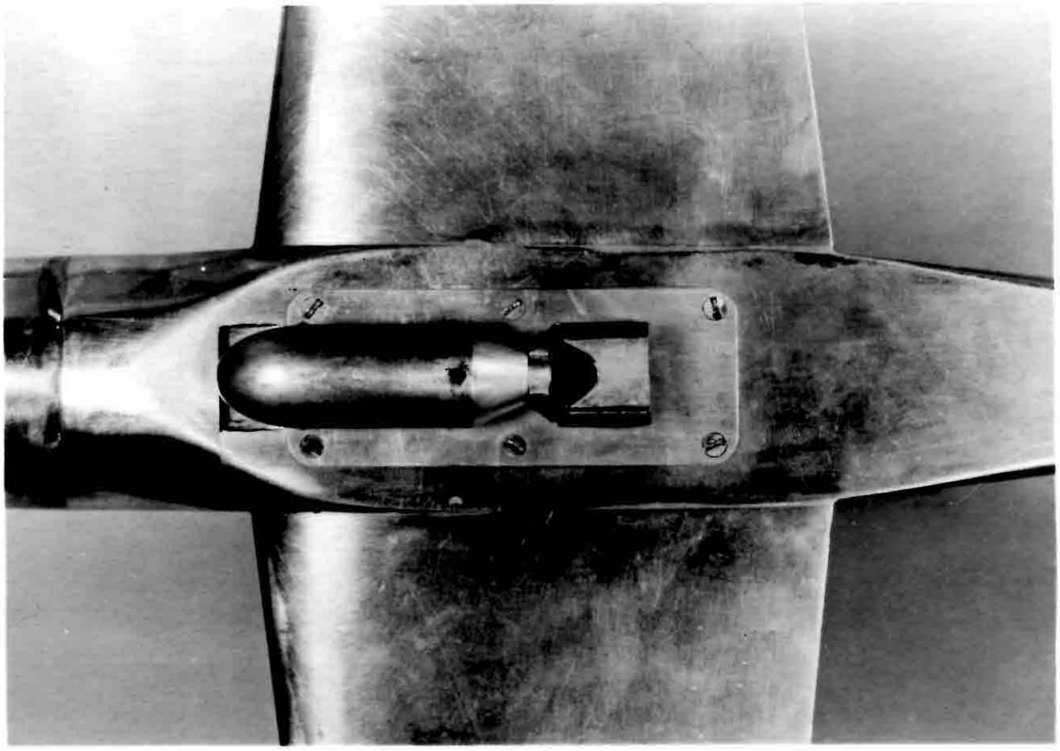

FIG. 4 — RELATION OF BOMB TO AIRFLOW OUTLET

POLARIZED LIGHT FLUME TESTS

Bentonite, suspended in the water of the Polarized Light Flume, has the property of streaming double refraction. When viewed by polarized light the flow pattern becomes visible. Further details of the flow characteristics are obtainable from the action of threads on the end of probes. Figure 5 shows the flow pattern for the lower part of the entire model and, in greater detail around the bomb, when the attack angle of the wing was 4 degrees up (bomb + 15 degrees). Figure 6 is similar but for a zero attack angle. Separation in Figure 5 is limited, essentially, to the afterbody, interior and rear of the tail structure, and between the fuselage and bomb section from the beginning of the afterbody to the end of the tail. This type of afterbody and tail structure is known to produce conditions highly conducive to tail vibration.* Such vibration increases with velocity and has caused tail failures on models tested in the Water Tunnel, although not with the low velocities used in the Polarized Light Flume.

The separation zone is much extended in Figure 6 as the trail from the tail moves up and follows along the lower part of the fuselage and bomb body forward of the afterbody.

*"Force Tests of Concrete Practice Bombs, M38A2 Practice Bomb, AN-M43 G. P. 500 lb. Bomb, AN-M56 L. C. 4000 lb Bomb", Section No. 6.1-sr207-2245, August 14, 1945.

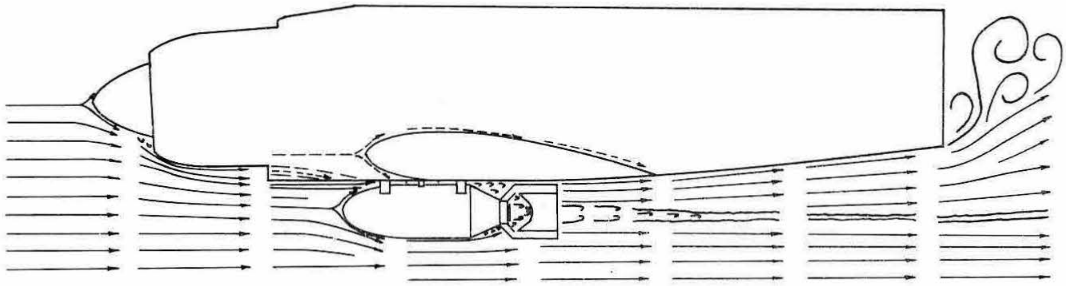

FIG. 5(A) — FLOW LINES AROUND AIRPLANE AND BOMB
WING ATTACK ANGLE — 4° UP

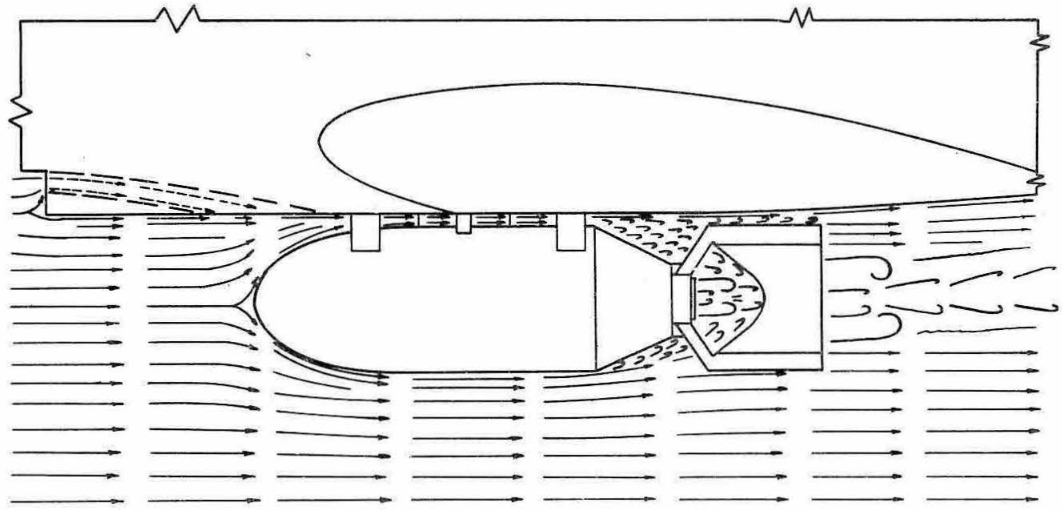

FIG. 5(B) — FLOW LINES AROUND BOMB
WING ATTACK ANGLE — 4° UP

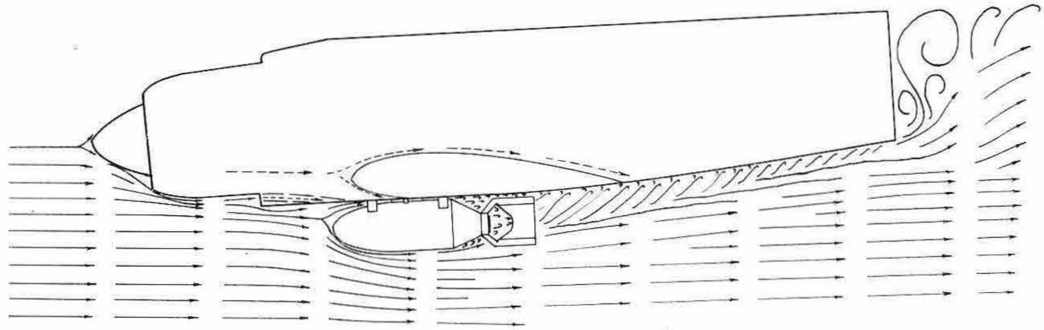

FIG. 6(A) — FLOW LINES AROUND AIRPLANE AND BOMB
WING ATTACK ANGLE — 0°

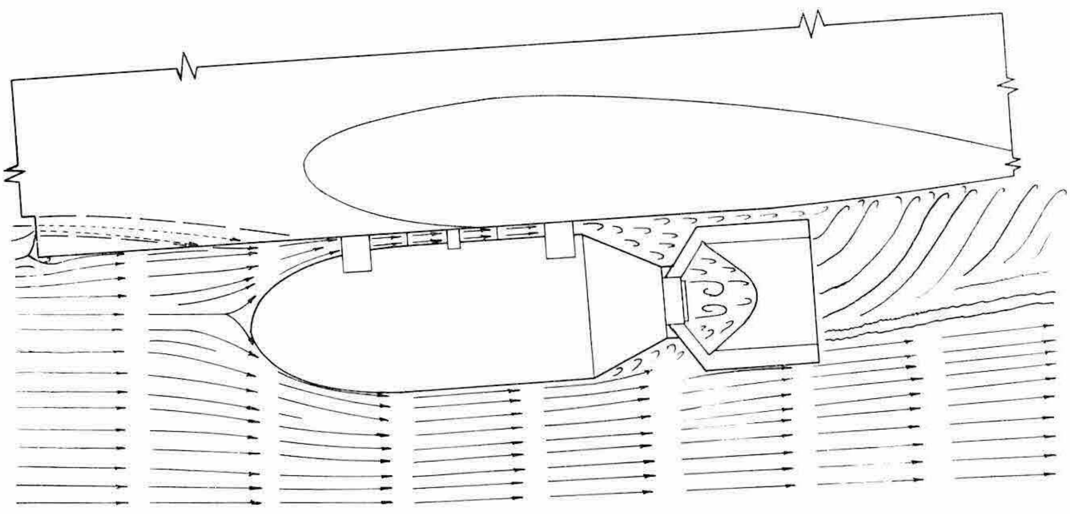

FIG. 6(B) – FLOW LINES AROUND BOMB
WING ATTACK ANGLE – 0°

CAVITATION TESTS

The original model tail came loose and was lost almost immediately and before any cavitation readings were taken. It was being observed for characteristics in a preliminary run. Cavitation had reached a stage, estimated from subsequent runs to have a K value about 1.00, which would correspond to some cavitation on tail surfaces, when the tail came off, presumably from excessive vibration. The metal of this tail was 0.006 inch thick, corresponding to prototype dimensions. A second tail was made to the same dimensions except that the metal thickness was doubled (0.012). This second tail withstood all subsequent tests but had, of course, greater stiffness and strength than the proper original.

Values of K for incipient cavitation were as follows:

Location	Wing Attack Angle, 4° Bomb Attack Angle, +15'	Wing Attack Angle, 30' Bomb Attack Angle, $-3^{\circ}15'$
Forward Struts	2.326	2.412
Forward Lug	1.697	1.733
Ejector	1.323	1.518
Rear Lug	1.289	1.416
Rear Struts	1.260	1.212
Tail, inside	1.137	0.994
leading edge	1.115	--
Afterbody	0.882	1.029
Nose	0.643	0.623

CAVITATION PHOTOGRAPHS

Figure 7 shows the development of cavitation on this model for the +15' bomb attack angle; Figure 8, for the -3° 15' bomb attack angle. The K values corresponding are indicated.

Figure 7 (a). K = 1.872. The cavitation at the rear of the forward strut is hardly visible in the photograph. A small light spot behind the strut and showing against the bomb body is all that may be seen readily. A small microscope reveals more bubbles on the strut near the bomb.

Figure 7(b). K = 1.507. Cavitation bubbles are now clearly evident on forward struts and trailing from forward lug.

Figure 7(c). K = 1.138. All struts, lugs, and ejector show cavitation. The small bubble trail above the afterbody has broken away from parts forward and is not originating on the afterbody.

Figure 7(d). K = 0.814. Afterbody cavitation. There is also cavitation on the inside of the tail and on leading edges which does not show in the photograph.

Figure 7(e). K = 0.772. A small microscope will reveal a line of cavitation inside the tail on the curved edge away from the observer.

Figure 7(f). K = 0.601. Cavitation streamers showing on nose. There appeared to be some pulsation of the cavitation between fuselage and bomb under these conditions.

Figure 7(g). K = 0.574. Further development of cavitation.

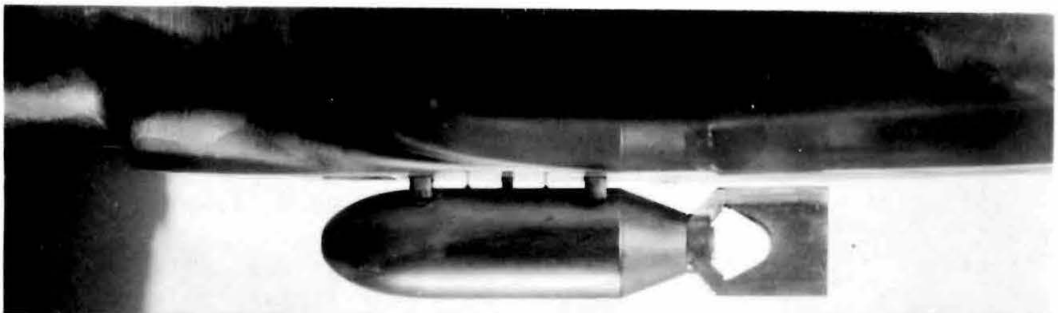

(a)

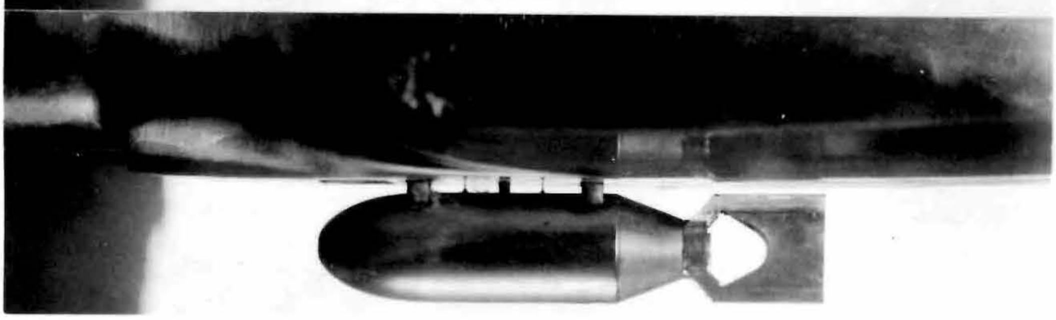

(b)

FIG. 7 — DEVELOPMENT OF CAVITATION FOR ATTACK ANGLE OF + 15'

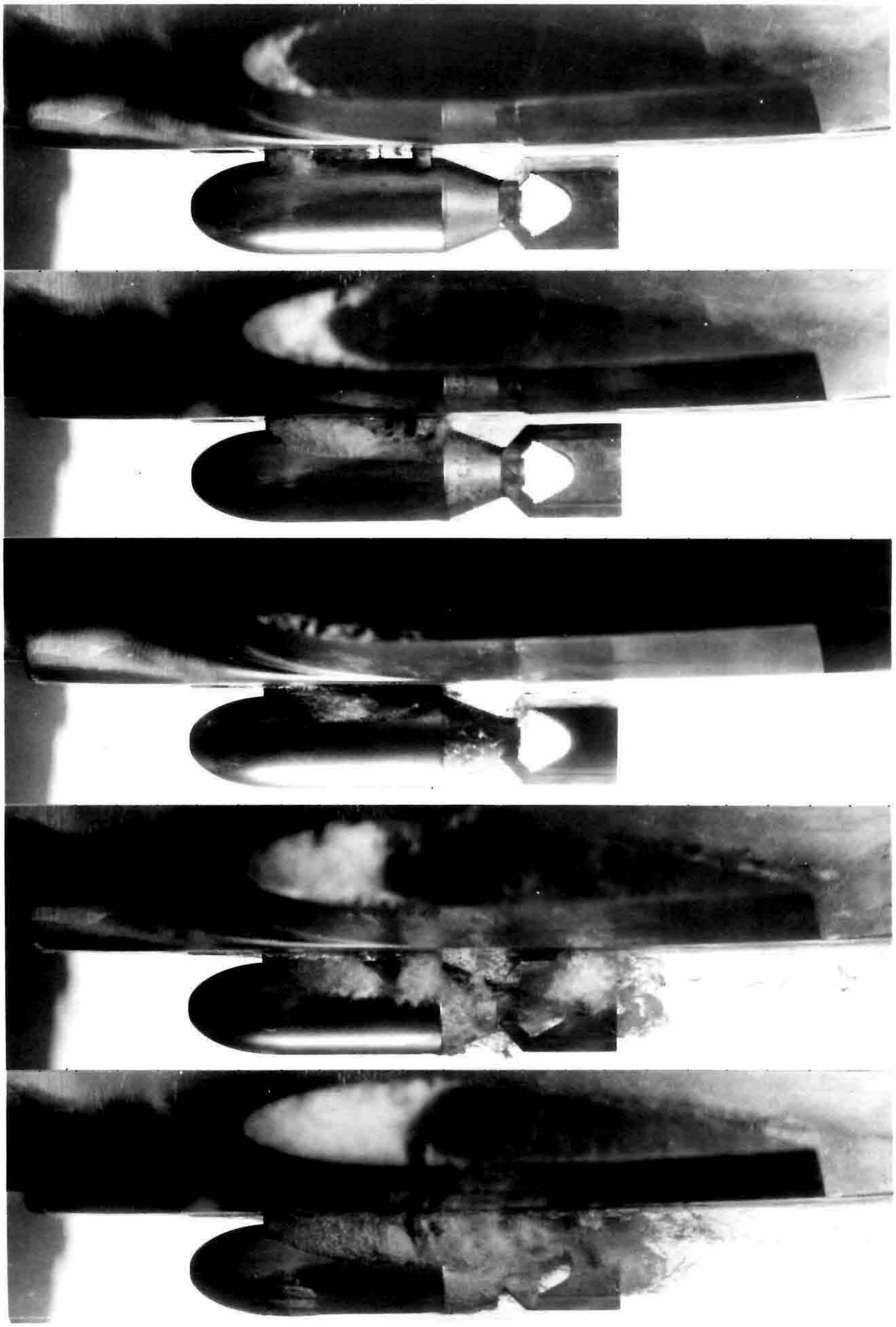

(c)

(d)

(e)

(f)

(g)

FIG. 7 (CONTINUED)

Figure 8(a). K = 1.703. Forward struts and lug.

Figure 8(b). K = 1.518. Incipient on ejector. Cavitation bubbles to rear of ejector have broken away from forward lug.

Figure 8(c). K = 1.212. Incipient on rear strut and showing on all forward appurtenances.

Figure 8(d). K = 0.994. Afterbody cavitation showing. Incipient inside tail but not showing.

Figure 8(e). K = 0.795. Further development.

Figure 8(f). K = 0.597. Nose cavitation plainly visible.

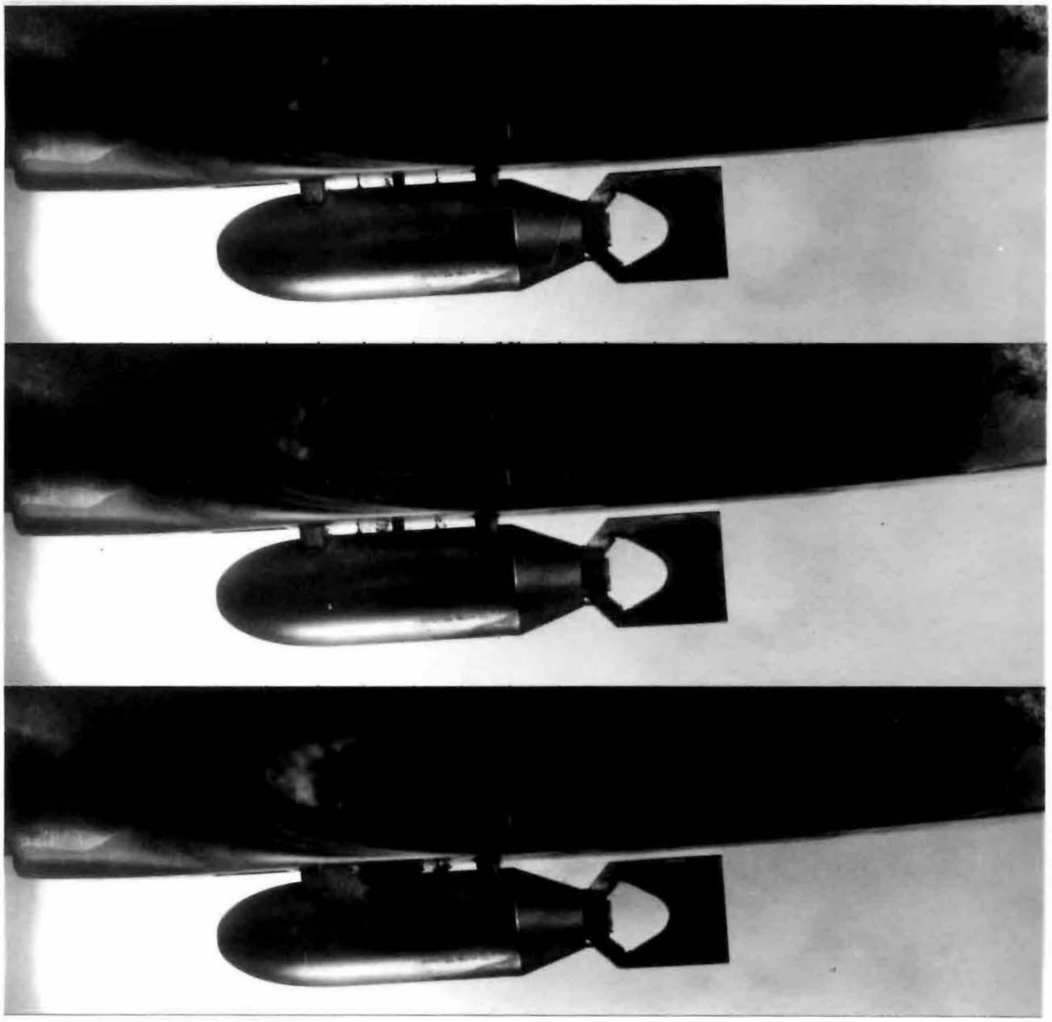

(a)

(b)

(c)

FIG. 8 — DEVELOPMENT OF CAVITATION WITH ATTACK ANGLE -3° 15'

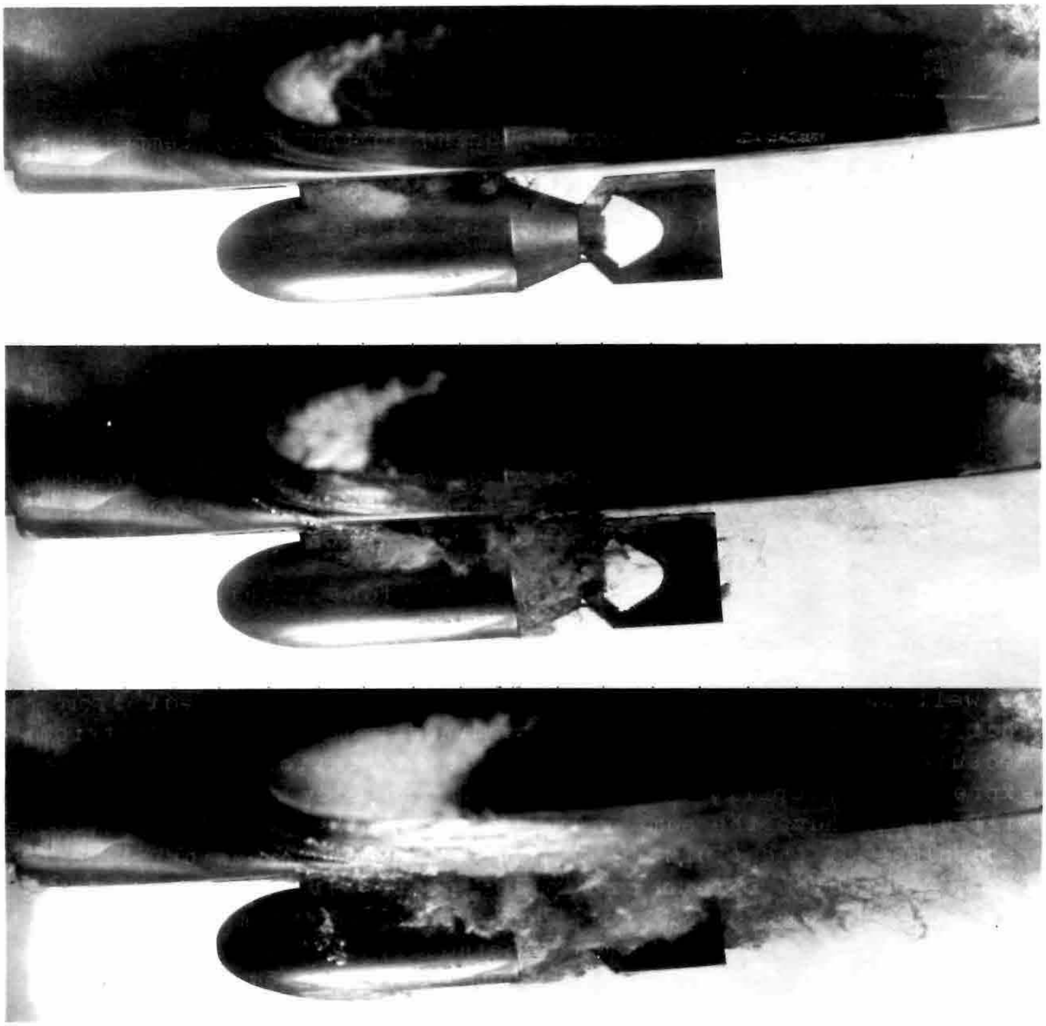

(d)

(e)

(f)

FIG. 8 (CONTINUED)

RELATIONS BETWEEN CAVITATION AND COMPRESSIBILITY

Cavitation occurs on the surface of a body moving through a liquid when the pressure at some point on the surface reaches the vapor pressure of the liquid. For streamlined bodies the minimum pressure in the fluid always occurs at the boundary of the body so that we can expect cavitation always to occur on the surface. The flow conditions for incipient cavitation are described in terms of the cavitation parameter, K, which is defined as

$$K = \frac{p_L - p_R}{\rho \frac{v^2}{2}} \qquad (1)$$

where

p_L = absolute pressure in the undisturbed liquid, lbs/sq ft

p_B = vapor pressure corresponding to the water temperature, lbs/sq ft

v = velocity of the projectile, ft/sec

ρ = mass density of the fluid in slugs/cu ft = w/g

w = weight of the fluid in lbs/cu ft

g = acceleration of gravity in ft/sec^2

Equation (1) states that when vapor pressure is reached at some point on the body, the difference in pressure between the undisturbed liquid and the minimum pressure on the body divided by the dynamic pressure $\rho \frac{v^2}{2}$ is a constant. This relation also holds when the pressure on the body is greater than vapor pressure, so that we can think of the quantity K as a pressure coefficient as well as a cavitation parameter. It is also clear from this that the quantity K could be determined from pressure distribution measurements as well as from direct cavitation observations. K expresses a property of the shape of the body since a given shape will always have the same value of K or of the pressure coefficient regardless of the fluid it is in as long as compressibility effects are negligible. Since cavitation starts at the point of lowest pressure, it also occurs at the point of maximum local velocity, as can easily be shown from the Bernoulli equation. In a compressible fluid the compressibility burble starts at the point where the local velocity is a maximum. Therefore, cavitation and the compressibility burble will form at the same place on a given shape. The local velocity on a given shape in a compressible fluid is expressed in terms of a coefficient of pressure, which is defined by the equation

$$C_P = \frac{p_1 - p}{\rho \frac{v^2}{2}} \tag{2}$$

where

p_1 is the pressure in the undisturbed fluid

p is the pressure at a point on the surface of the body

ρ is the density of the fluid

v is the velocity of the body relative to the fluid

In deriving the equations it is convenient to express the velocities as ratios to the velocity of sound in the fluid. This ratio is called the Mach number. In a relatively incompressible fluid such as water, the value of the pressure coefficient is constant and independent of the value of the pressure and velocity; however, in a compressible fluid the pressure coefficient varies with pressure and velocity. The variation of this coefficient is expressed in the terms of the Mach number as follows:

$$C_{p_M} = \frac{2(p - p_1)}{\rho_1 v_1^2} = C_{p_o} \frac{1}{\sqrt{1 - M_1^2} + \frac{M_1^2}{1 + \sqrt{1 - M_1^2}} \frac{C_{p_o}}{2}} \tag{3}$$

Here the Mach number M_1 is the ratio between the velocity of the undisturbed flow relative to the body and the velocity of sound in the fluid, and the C_{p_o} is the pressure coefficient for a point on the body for Mach number zero. For our purposes the value of C_{p_o} can be taken as equivalent to the value of K for incipient cavitation since in the Water Tunnel the value of the Mach number is very small. The values of C_{p_M} for various values of C_{p_o} are given by the family of relatively horizontal curves in Figure 9.

When the local velocity at a point on the body reaches the sonic velocity, a compressibility burble will form. This condition will be reached for a certain critical value of the pressure coefficient C_{p_M} which is denoted as $(C_p)_{cr}$ and defined by

$$\left(C_p\right)_{cr} = \frac{p_1 - p}{\rho_1 \frac{v_1^2}{2}} = \frac{2}{\gamma M_1^2}\left(1 - \frac{p}{p_1}\right)$$

$$= \frac{2}{\gamma M_1^2}\left[1 - \left(\frac{2}{\gamma + 1}\right)^{\frac{\gamma}{\gamma - 1}} \left(1 + \frac{\gamma - 1}{2} M_1^2\right)^{\frac{\gamma}{\gamma-1}}\right] \tag{4}$$

where the quantity, γ, is the ratio of the specific heats of the fluid. The development of this formula is given in Appendix A, and was obtained from the book "Introduction to Aerodynamics of a Compressible Fluid," Liepmann and Puckett, Galcit Aeronautical Series, Wiley and Sons, 1947.

When γ is taken as 1.405 for air, the formula becomes

$$\left(C_p\right)_{cr} = \frac{1 - (0.5282)\ (1 + 0.2025\ M^2)^{3.47}}{0.7025\ M^2} \tag{5}$$

This formula (5) gives the full line, relatively vertical and intersecting the family of lines, shown in Figure 9. The points shown and the dash line portion are as given by von Karman in Figure 13 of the article entitled "Compressibility Effects in Aerodynamics," Theodore von Karman, Journal of the Aeronautical Sciences, Vol. 8, No. 9, July, 1941. The correspondence below M = 0.7 is seen to be close. The intersection values were converted to velocity in miles per hour on a basis of 758 miles per hour for M = 1 and plotted against the corresponding K values at critical velocity. (The test K values were at very low Mach number - about 0.026.) The resultant curve appears as Figure 10.

DISCUSSION OF RESULTS

From Figure 10 and the incipient K values listed above, it may be seen that the critical Mach number is predicted for the various parts listed at the approximate velocities shown below:

Location	Speed, mi/hr	
	Wing Attack Angle, 4° Bomb Attack Angle, +15°	Wing Attack Angle, 0° Bomb Attack Angle, -3°45'
Forward Struts	not obtained but less than 300	
Forward lug	357	354
Ejector	401	378
Rear lug	405	391
Rear struts	409	416
Tail, inside	426	446
leading edge	429	--
Afterbody	462	441
Nose	502	506

The model tested is most nearly comparable to the full-scale test of the standard 2,000 lb. bomb with stiffened fins. The Douglas Aircraft Company report indicated that this bomb did not give objectionable buffeting until the air speed was 440 mi/hr. Since the list above shows that all struts, lugs, and the ejector cavitate heavily at speeds considerably less, the conclusion appears to be justified that the attainment of critical Mach numbers is not, in itself, necessarily an essential factor in objectionable buffeting. When cavitation begins on the tail surfaces, a violent vibration may, and in this case does, occur. It appears then that the buffeting is primarily a result of the transfer of this vibration to the control surfaces through the air stream or airplane strusture or both. The reduction of tail vibration may be obtained by mechanical resistance to vibration and/or a design which minimizes its inception.

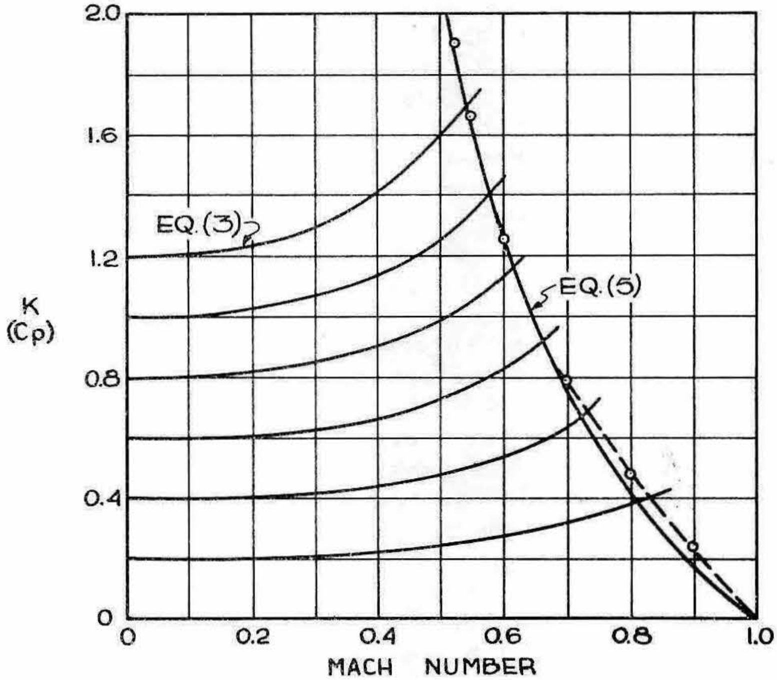

FIG. 9 - CRITICAL MACH NUMBERS FOR VARIOUS K'S

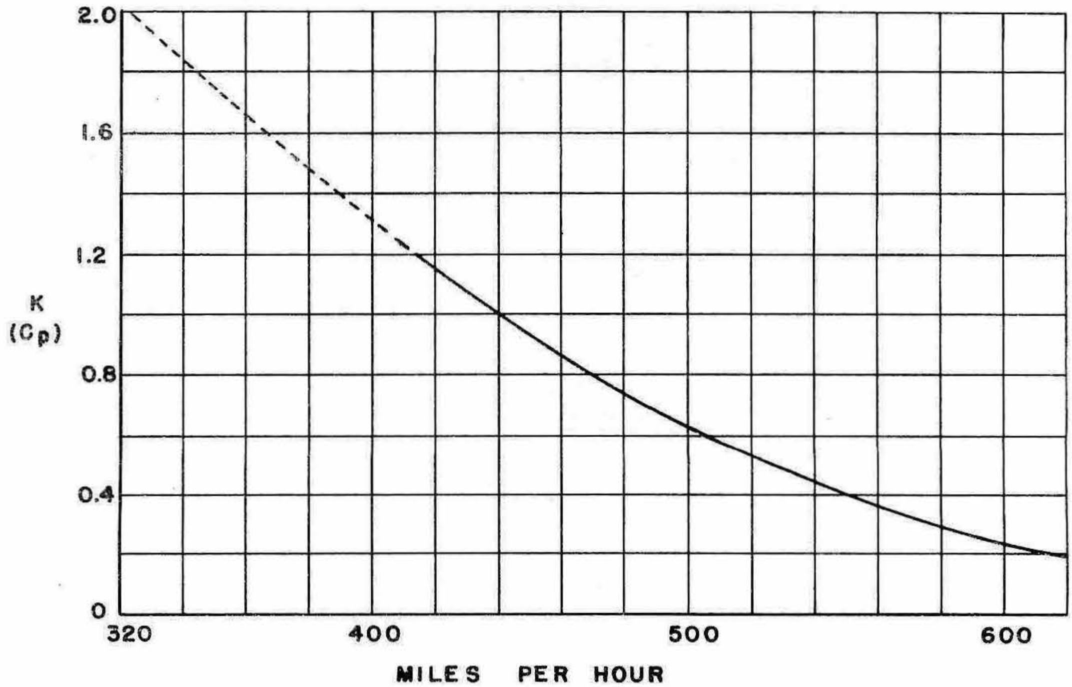

FIG. 10 - CRITICAL SPEEDS FOR VARIOUS K VALUES

While it thus appears that incipient cavitation should predict the velocity for which the local velocities on the surface of the body reach the sonic, there is, as yet, no basis apparent for evaluating the quantitative effects such local sonic velocities would have upon performance nor to predict any effects resulting from speeds in excess of the critical speed by studying cavitation beyond the incipient stage.

CONCLUSIONS

1. Sonic velocities in small localized zones do not seem, in themselves, to cause objectionable buffeting.

2. Sonic velocities may set up violent vibration in surfaces such as bomb tail fins and, when this occurs, it may be transferred in an objectionable degree to control surfaces. This may be corrected by stiffening the parts which tend to vibrate or by improvement in their design.

3. It appears that Polarized Light Flume studies can contribute only slightly to the solution of problems of this nature.

4. Cavitation studies in the High Speed Water Tunnel apparently do serve to determine the flow at which sonic velocity is reached at various points on a given body.

5. Such studies do not, currently, provide a basis for evaluating the quantitative effect of such local sonic velocities nor to predict any effects resulting from speeds in excess of the critical speed by studying cavitation beyond the incipient stage.

APPENDIX A

Derivations of Equations Used

Symbols

a = local speed of sound in a fluid, feet per second

a^* = critical velocity, feet per second

C = specific heat

C_p = specific heat at constant pressure

C_v = specific heat at constant volume

M = Mach number $= \frac{u}{a}$. Dimensionless

p = pressure, lbs/sq ft

p_o = pressure for initial conditions

p_1, p_2 = pressure at points 1, 2

R = gas constant

T = temperature, degrees Rankine. Zero is at $-460^{\circ}F$

T_o = temperature for initial conditions

T_1, T_2 = temperatures at points 1, 2

u = velocity of stream, ft/sec

u_o = initial velocity

u_1, u_2 = velocity at points 1, 2

v = specific volume, cu ft/slug

$= \frac{C_p}{C_v}$. Taken as 1.405 for air

ρ = density, slugs/cu ft

ρ_o = initial density

ρ_1, ρ_2 = density at points 1, 2

Standard textbooks give the following basic relations:

$P = \rho RT$ (equation of state) or $T = \dfrac{p}{\rho r}$

$Pv = RT$

$C_p = R + C_v$

$\gamma = \dfrac{C_p}{C_v}$

Then $C_v = \dfrac{C_p}{\gamma}$ and $C_p = R + \dfrac{C_p}{\gamma}$

$$R = C_p - \frac{C_p}{\gamma} = \frac{\gamma C_p - C_p}{\gamma} = \frac{C_p\ (\gamma - 1)}{\gamma}$$

$$T = \frac{p}{\rho} \times \frac{\gamma}{C_p\ (\gamma - 1)} = \frac{p}{C_p \rho} \left(\frac{\gamma}{\gamma - 1}\right)$$

The energy equation for a perfect gas is also given as

$$\frac{u^2}{2} + C_p T = C_p\ T_o$$

Substituting appropriate values for T and T_o gives

$$\frac{u^2}{2} + C_p \left(\frac{p}{C_p \rho} \quad \frac{\gamma}{\gamma - 1}\right) = C_p \left(\frac{p_o}{C_p\ \rho_o} \quad \frac{\gamma}{\gamma - 1}\right)$$

which becomes

$$\frac{u^2}{2} + \frac{\gamma}{\gamma - 1} \frac{p}{\rho} = \frac{\gamma}{\gamma - 1} \frac{p_o}{\rho_o}$$

or

$$\frac{u^2}{2} + \frac{1}{\gamma - 1} \frac{\gamma p}{\rho} = \frac{1}{\gamma - 1} \frac{\gamma\ p_o}{\rho_o}$$

It can also be shown that

$$\frac{dp}{p} = \gamma \frac{dp}{\rho} \quad \text{or} \quad \frac{dp}{d\rho} = \frac{\gamma \cdot p}{\rho}$$

Now $\dfrac{dp}{d\rho} = a^2 = \dfrac{\gamma\ p}{\rho}$ so a^2 can be substituted for $\dfrac{\gamma\ p}{\rho}$

in the formula above, giving

$$\frac{u^2}{2} + \frac{1}{\gamma - 1} a^2 = \frac{1}{\gamma - 1} a_o{}^2$$

where a_o is the speed of sound in the reservoir from which the flow at speed u_2 issues. If we divide this equation by

$\frac{a^2}{\gamma -1}$ it takes the following dimensionless form

$$\frac{\gamma -1}{2}\left(\frac{u}{a}\right)^2 + 1 = \left(\frac{a_o}{a}\right)^2$$

Using the fact that $\left(\frac{a}{a_o}\right)^2 = \frac{T}{T_o}$

this can be written

$$\frac{T_o}{T} = 1 + \frac{\gamma - 1}{2} M^2 \quad (\text{since } \frac{u}{a} = M)$$

If the flow is isentropic, that is, a reversible adiabatic process, the pressure, density, and temperature may be related to these speed ratios. The last equation above relates the temperature ratio to the local Mach number, M, and in isentropic flow, the pressure ratio is a particular function of the temperature

$$\left(\frac{a_o}{a}\right)^2 = \frac{T_o}{T} = \left(\frac{p_o}{p}\right)^{(\gamma-1)/\gamma}$$

Therefore, by substituting the value of $\frac{T_o}{T}$, above, we get

$$\frac{p_o}{p} = \left(1 + \frac{\gamma - 1}{2} M^2\right)^{\gamma/(\gamma-1)}$$

Let the free stream speed in a certain flow be less than the local speed of sound. If there is a body in the flow around which the pressure drops below its free stream value, the air will be accelerated and may reach the speed of sound. The additional necessary pressure drop to produce this may be found. Let M_1 and p_1 be the Mach number and the pressure in the free stream, then

$$\frac{p_o}{p_1} = \left(1 + \frac{\gamma - 1}{2} M_1^2\right)^{\gamma/(\gamma-1)}$$

If, at the second point $M_2 = 1$ and the pressure is p_2.

$$\frac{p_o}{p_2} = \left(1 + \frac{\gamma - 1}{2}\right)^{\gamma/(\gamma-1)}$$

Then $p_1 \left(1 + \frac{\gamma - 1}{2} M_1^2\right)^{\gamma/(\gamma-1)} = p_2\left(1 + \frac{\gamma - 1}{2}\right)^{\gamma/(\gamma-1)}$

and $$\frac{p_2}{p_1} = \frac{\left(1 + \frac{\gamma - 1}{2} M_1^2\right)^{\gamma/(\gamma-1)}}{\left(1 + \frac{\gamma - 1}{2}\right)^{\gamma/(\gamma-1)}}$$

$$= \left(\frac{1 + \frac{\gamma - 1}{2} M_1^2}{\frac{\gamma+1}{2}} \right)^{\gamma/(\gamma - 1)}$$

This may be transformed to a pressure coefficient

$$C_p = \frac{p_2 - p_1}{q_1}$$

Now $q = 1/2\ \rho\, u^2$ since $\frac{u}{a} = M$, $u^2 = M^2\, a^2$

and $a^2 = \frac{\gamma\, p}{\rho}$ from above, so $u^2 = \frac{M^2\, \gamma\, p}{\rho}$

Then $q = 1/2\ M^2\, \gamma\, p$

Whereupon $C_p = \frac{p_2 - p_1}{1/2\ M_1^2\, \gamma\, p_1} = \frac{p_2 - p_1}{p_1} \frac{2}{\gamma\, M_1^2}$

Therefore

$$C_p \text{ crit} = \frac{2}{\gamma\, M_1^2} \left(\frac{p_2 - p_1}{p_1} \right)$$

$$= \frac{2}{\gamma\, M_1^2} \left(\frac{p_2}{p_1} - 1 \right)$$

Substituting the value of $\frac{p_2}{p_1}$ gives, after simplifying,

$$C_p \text{ crit} = \frac{2}{\gamma\, M_1^2} \left[\left(\frac{2}{\gamma + 1} + \frac{\gamma - 1}{\gamma + 1} M_1 2 \right)^{\gamma/(\gamma-1)} -1 \right]$$

If we call the normal values of pressure, density, velocity, and Mach number p_1, ρ_1, u_1, and M_1, respectively, this may be rewritten in another form as

$$\left(C_p \right)_{cr} = \frac{p_1 - p}{1/2\ \rho_1 u_1^2} = \frac{2}{\gamma\, M_1^2} \left(1 - \frac{p}{p_1} \right)$$

$$= \frac{2}{\gamma\, M_1^2} \left[1 - \left(\frac{2}{\gamma + 1} \right)^{\gamma/(\gamma - 1)} \left(1 + \frac{\gamma - 1}{2} M_1^2 \right)^{\gamma/(\gamma-1)} \right]$$

which was the formula used.